Journal of Automation and Control Engineering Vol. 1, No. 3, September 2013

Performance Improvement Technique for Induction Motor Driven by a Matrix Converter under Abnormal Input Conditions

Nguyen Khanh Tu Tam, Nguyen Van Nho, Huynh Thai Hoang, and Vu Duy Nhat
Faculty of Electrical & Electronics Engineering, Ho Chi Minh city University of Technology
268 Ly Thuong Kiet Street, Ward 14, District 10, Ho Chi Minh City, VietNam
Email: tam_nguyen_bk@yahoo.com

***Abstract*—Matrix converter (MC) is an AC-AC power converter topology that directly converts energy from AC source to an AC load without using any energy storage components. Therefore, the disturbances in the input voltages can propagate onto the output side and degrade or even deteriorate the performance of motor load. This paper investigates the behavior of MC and its influence to the performance of induction motor under unbalanced input condition. A feed-forward compensation technique to eliminate the output voltage distortion of MC and ensure the proper operation of induction motor under unbalance is then proposed. Effectiveness and feasibility of the compensation method has been demonstrated through simulation results.**

***Index Terms*—Matrix converter, induction motor, unbalance, sensorless control**

I. Introduction

Three phase matrix converter have received considerable attention in recent years [1]-[4], and some have been produced commercially. MC possesses high quality performances such as near sinusoidal input/output waveforms, adjustable input power factor and compact system design. Therefore, the induction motor driver fed by matrix converter is more advantageous to the conventional inverter. However, due to the lack of the dc-link storage component, MC is much more susceptible to the input voltage disturbances. If the induction motor is used as a load of MC, any disturbance in the AC source voltage will be immediately reflected to the stator and thus unwanted ripple will appear in the electromagnetic torque. This will lead to the degradation and even deterioration of the system performance.

In order to cope with this problem, several techniques that reduce the influence of abnormal input voltages for MC have been presented in some papers [2]-[4]. Paper [2], [3] are based on a dynamic modulation of the instantaneous displacement angle between input voltage and current vectors in the direct conversion scheme. In paper [4], the conversion process is fictitiously divided into rectification and inversion states, the compensation technique is carried out by adjusting the voltage source inverter (VSI) modulation index m_v .

In this paper, the influence of abnormal input voltages to a system of induction motor driver fed by MC will be analyzed in detail. The MC will be controlled with the same indirect space vector modulation in [4], and a feed-forward compensation technique with a modified input displacement factor (IDF) control is proposed. This IDF control strategy, together with the adjusted modulation index, will ensure reliable operation for the MC under unbalance.

A sensorless vector control is utilized as the control algorithm for the induction motor. To improve the low speed operation performance, the adaptive full order observer with high accuracy in stator flux, rotor speed and stator resistance estimation is employed. This control scheme can also be found in [6]-[8]. The output waveforms of the MC and the instantaneous electromagnetic torque, speed response of the induction motor in uncompensated and compensated system will be shown through simulation to verify the effectiveness of the feed-forward compensation strategy.

II. MC Control Strategy

A three phase to three phase matrix converter consists of nine bi-directional switches which allow any output phase A, B, C to be connected to any input phase, as shown in Fig. 1.

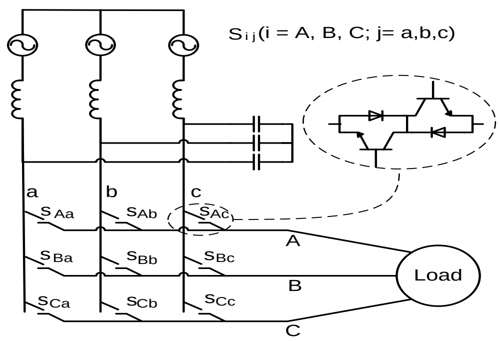

Figure 1 The topology of three-phase to three phase matrix converter

Manuscript received Oct. 31, 2012; revised Jan 28, 2013.

doi: 10.12720/joace.1.3.186-191

The input phase voltages under normal condition can be express as:

$$\left[v_{iph}(t)\right]=\begin{bmatrix}v_a(t)\\v_b(t)\\v_c(t)\end{bmatrix}=V_{im}\begin{bmatrix}\cos(\omega_i t)\\\cos(\omega_i t-120^o)\\\cos(\omega_i t+120^o)\end{bmatrix}\qquad(1)$$

where V_{im} and ω_i are respectively the amplitude and input angular frequency of the input phase voltages.

In order to obtain the desirable sinusoidal average output line voltage, e.g.,

$$\left[v_o(t)\right]=\begin{bmatrix}\bar{v}_{AB}\\\bar{v}_{BC}\\\bar{v}_{CA}\end{bmatrix}=\sqrt{3}V_{om}\begin{bmatrix}\cos(\omega_o t-\varphi_o)\\\cos(\omega_o t-\varphi_o-120^o)\\\cos(\omega_o t-\varphi_o+120^o)\end{bmatrix}\qquad(2)$$

, a typical transfer function for MC is expressed in (3)

$$\left[M(t)\right]=m.\begin{bmatrix}\cos(\omega_o t-\varphi_o)\\\cos(\omega_o t-\varphi_o-120^o)\\\cos(\omega_o t-\varphi_o+120^o)\end{bmatrix}.\begin{bmatrix}\cos(\omega_i t-\varphi_i)\\\cos(\omega_i t-\varphi_i-120^o)\\\cos(\omega_i t-\varphi_i+120^o)\end{bmatrix}^T\qquad(3)$$

where $0\le m\le 1$ is the modulation index and φ_i is arbitrary angle.

As clearly proved in [1], this transfer function imitates *a VSR-VSI conversion, as shown in Fig. 2*

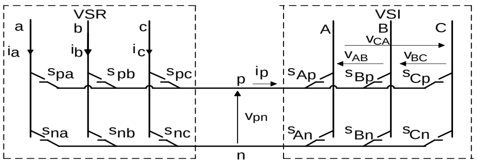

Figure 2 Emulation of VSR- VSI conversion

V_{pn} in Fig. 2 is a fictitious dc-link voltage which is calculated as

$$V_{pn}=V_{dc}=\frac{3}{2}V_{im}\cos\varphi_i\qquad(4)$$

As a result of the transfer function emulation, the sampled values of the desired output line voltage space vector and input phase current space vector defined by

$$\begin{aligned}\bar{v}_{oL}&=\sqrt{3}.V_{om}.e^{j(\omega_o t-\varphi_o)}=V_{oL}.e^{j\theta_o}\\ \bar{i}_i&=I_{im}.e^{j(\omega_i t-\varphi_i)}\quad=I_{im}.e^{j\theta_i}\end{aligned}\qquad(5)$$

can be synthesized by two adjacent switching state vectors and zero vectors in their respective hexagons using PWM technique as illustrated in Fig. 3.

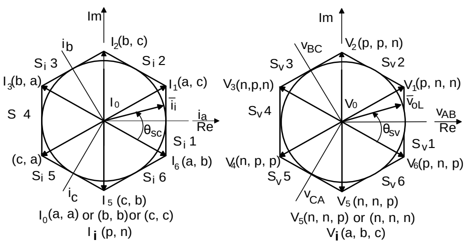

Figure 3 VSR hexagon (a) and VSI hexagon (b)

The simultaneous output voltage and input current SVM can be obtained by combining the two modulation strategies in both parts VSI and VSR of MC. Depending on location of the two rotating reference space vector $\bar{V}_{oL}$ and $\bar{i}_i$ in sectors of their respective hexagons, an appropriate set of switching combinations which on-times are determined as

$$\begin{aligned}&d_{\alpha\mu}=d_\alpha.d_\mu=T_{\alpha\mu}/T_s=m_c.m_v.\sin(60^o-\theta_{sv}).\sin(60^o-\theta_{sc}),\\&d_{\beta\mu}=d_\beta.d_\mu=T_{\beta\mu}/T_s=m_c.m_v.\sin(\theta_{sv}).\sin(60^o-\theta_{sc}),\\&d_{\alpha v}=d_\alpha.d_v=T_{\alpha v}/T_s=m_c.m_v.\sin(60^o-\theta_{sv}).\sin(\theta_{sc}),\\&d_{\beta v}=d_\beta.d_v=T_{\beta v}/T_s=m_c.m_v.\sin(\theta_{sv}).\sin(\theta_{sc}),\\&d_0\ =1-d_{\alpha\mu}-d_{\beta\mu}-d_{\alpha v}-d_{\beta v},\end{aligned}\qquad(6)$$

, will be selected. where m_c is the VSR modulation index and is chosen as 1 for simplicity. m_v is the VSI modulation index which defines the desired voltage transfer ratio from the DC link to the peak output voltage

$$0\le m_v=\sqrt{3}.V_{om}/V_{dc}\le 1\qquad(7)$$

III. Induction Motor Control Algorithm

A. Induction Motor Model

The general induction motor model in arbitrary reference frame is described as follows

$$\begin{aligned}u_s&=R_s i_s+d\psi_s/dt+j\omega_e\psi_s\\0&=R_r i_r+d\psi_r/dt+j(\omega_e-\omega_r)\psi_r\\\psi_s&=L_s i_s+L_m i_r\\\psi_r&=L_r i_r+L_m i_s\\T_e&=\frac{3}{2}P\frac{L_m}{L_r}\operatorname{Im}\{i_s\psi_r\}\end{aligned}\qquad(8)$$

where

u_s,u_r,i_s,i_r stator and rotor voltage and current vectors

$\psi_s,\ \psi_r$ stator and rotor flux linkage vector

L_s,L_m,L_r stator, magnetizing and rotor inductance

ω_e angular velocity of the rotor field with respect to the stator

ω_r angular velocity of the rotor

T_e electromagnetic torque expressed in terms of space vectors

B. Principle of Field-Oriented Controller

The main objective of the RFOC is to independently control the torque and flux. This is done by selecting the speed of the reference frame equal to the speed of rotation of rotor flux space vector. Under this condition, the rotor flux space vector becomes a pure real variable since

$$\psi_{dr}=\psi_r\ \text{and}\ \psi_{qr}=0\qquad(9)$$

The torque equation in (8) is then expressed in the following form:

$$T_e=\frac{3}{2}P\frac{L_m}{L_r}\psi_{dr}i_{qs}\qquad(10)$$

With an assumption that the operation is under constant flux region, the d-q components of stator voltage, can be simplified to

$$\begin{aligned}v_{ds}&=R_s i_{ds}+\sigma L_s di_{ds}/dt-\omega_r\sigma L_s i_{qs}\\v_{qs}&=R_s i_{qs}+\sigma L_s di_{qs}/dt+\omega_r L_s i_{ds}\end{aligned}\qquad(11)$$

where $\sigma=1-L_m^2/(L_sL_r)$

C. Sensorless Vector Control Using Adaptive Model

In order to achieve high accuracy in rotor speed, flux, and stator resistor estimation, an adaptive observer that offers good performance in a large speed range is employed. Equation of states estimation in the stationary frame is expressed as:

$$\frac{d}{dt}\hat{x} = \hat{A}\hat{x} + Bu_s + G(\hat{i}_s - i_s) = \begin{bmatrix} \hat{A}_{11} & \hat{A}_{12} \\ \hat{A}_{21} & \hat{A}_{22} \end{bmatrix}\hat{x} + \begin{bmatrix} B_1 \\ O_2 \end{bmatrix} u_s + G(\hat{i}_s - i_s) \tag{12}$$

where

$\hat{x} = [\hat{i}_{s\alpha}\ \hat{i}_{s\beta}\ \hat{\psi}_{r\alpha}\ \hat{\psi}_{r\beta}]^T$: estimated values of stator currents and rotor flux on stationary frame

$u_s = [u_{s\alpha}\ u_{s\beta}]^T$, $i_s = [i_{s\alpha}\ i_{s\beta}]^T$: stator voltages and currents

$$\hat{A}_{11} = (-\hat{R}_s/(\delta L_s) + (1-\delta)/(\delta T_r))I = a_{r11}I$$
$$\hat{A}_{12} = L_m/(\delta L_s L_r)((1/T_r)I - \hat{\omega}_r J) = a_{r12}I + a_{i12}J$$
$$\hat{A}_{21} = (L_m/T_r)I = a_{r21}I$$
$$\hat{A}_{22} = (-1/T_r)I + \hat{\omega}_r J = a_{r22}I + a_{i22}J$$
$$I = \begin{bmatrix} 1 & 0 \\ 0 & 1 \end{bmatrix}, J = \begin{bmatrix} 0 & -1 \\ 1 & 0 \end{bmatrix}, B_1 = (1/\delta L_s)I, O_2 = \begin{bmatrix} 0 & 0 \\ 0 & 0 \end{bmatrix}$$

T_r is the rotor time constant, $\hat{\omega}_r$ is the estimated speed G is the feedback gain of the observer, G is selected so that the pole location of the observer is k times ($k \geq 1$) proportional to the motor poles [5]:

$$G = \begin{bmatrix} g_1 & g_2 & g_3 & g_4 \\ -g_2 & g_1 & -g_4 & g_3 \end{bmatrix}^T$$

where

$$g_1 = (k-1)(\hat{a}_{r11} + \hat{a}_{r22}) \quad , \quad g_2 = (k-1)\hat{a}_{i22}$$
$$g_3 = (k^2-1)(\hat{a}_{r21} - \rho\hat{a}_{r11}) + \rho g_1 \text{ , } g_4 = \rho g_2$$
$$\rho = -(L_s L_r - L_m^2)/L_m$$

The adaptive schemes for speed and stator resistance estimation are described as

$$\omega_r = K_{p\omega}\left(e_{s\alpha}\psi_{r\beta} - e_{s\beta}\psi_{r\alpha}\right) + K_{i\omega}\int\left(e_{s\alpha}\psi_{r\beta} - e_{s\beta}\psi_{r\alpha}\right)dt$$
$$\hat{R}_s = -K_{pr}\left(e_{s\alpha}i_{s\alpha} + e_{s\beta}i_{s\beta}\right) - K_{ir}\int\left(e_{s\alpha}i_{s\alpha} + e_{s\beta}i_{s\beta}\right)dt$$

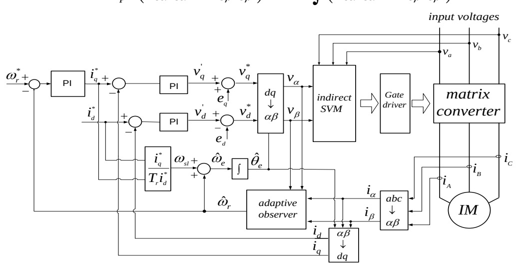

Figure 4 System configuration of sensorless vector control of induction motor driven by matrix converter

IV. Performance of System of Matrix Converter Fed Induction Motor under Abnormal Input Condition

A. Matrix Converter Operation under Abnormal Input Voltages

The dc-link voltage described in (4) supplies directly to the VSI part in the VSR-VSI conversion illustrated in Fig. 2. When utilizing the SVM for the VSI part, under normal condition of input voltages, this dc-link voltage is always considered to be a constant value. Thus, any variation of this voltage will be reflected to the output if the SVM is employed without any compensation technique.

To analyze the dc-link voltage variation due to the abnormal input voltages, a more general equation is proposed

$$V'_{pn} = V'_{dc} = \frac{3}{2}|\overline{v}_i|\cos(\theta_e - \theta_i) = \frac{3}{2}|\overline{v}_i|\cos\varphi'_i \tag{13}$$

where $|\overline{v}_i|$ is the magnitude of input phase voltage space vector, φ'_i is the generalized input displacement factor.

In normal input conditions, $\overline{v}_i$ has a constant magnitude and rotates at a constant angular velocity ω_i. Since

$$\begin{cases} |\overline{v}_i| = V_{im} \\ \varphi'_i = \theta_e - \theta_i = \varphi_i \end{cases} \tag{14}$$

, (13) and (4) are thus equivalent.

However, under abnormal conditions in terms of input unbalance, non-sinuisoidal input voltages and short time voltage sags, magnitude and angular velocity of $\overline{v}_i$ are no longer constant and (14) is no longer satisfied. In this case, (13) provides an accurate result of dc-link voltage variation while (4) always produces a constant value as in normal condition. This leads to the wrong operation for MC since (4) is used to derive the SVM for VSI part of the imaginary VSR-VSI in Fig. 2.

To illustrate the performance of MC under normal and abnormal input conditions, simulation results of two cases are given:

Case 1: Balanced and sinuisoidal input voltages which magnitude and frequency are 220Vrms and 50 Hz respectively.

Case 2: Abnormal input voltages created by adding 10% of third harmonic and 20% of fifth harmonic in each phase of the voltages in case 1.

In both cases, the desirable IDF is zero.

Fig. 5a and 5b illustrates respectively the variation in magnitude of input phase voltage space vector in case 1 and case 2. It is clear that the magnitude is constant in case 1 and time-varied in case 2.

Angular velocity of input phase voltage and current space vector and their deviation are observed in the same scope as shown in Fig. 6a for case 1 and 6b for case 2. The deviation is expected to be equal to the IDF which is set at zero in both cases. However, as clearly shown in Fig. 6a and Fig. 6b, the deviation is only equal to zero in case 1 while oscillating around zero in case 2.

The values of the dc-link voltage calculated by (4) and (13) are then plotted on the same graph as shown in Fig. 7a and Fig. 7b.

It can be seen that the dc-link voltage calculated by (13) is just equal to which calculated by (4) in case 1 while is different in case 2.

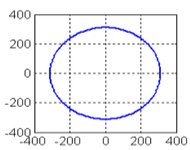

(a) Case 1

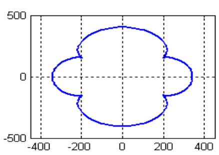

(b) Case 2

Figure 5 Magnitude variation of input phase voltage space vector under normal input voltages (Case 1) and abnormal input voltages (Case 2)

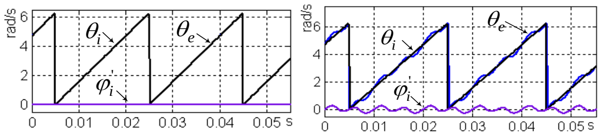

(a) Case 1 (b) Case 2

Figure 6 Angular velocity of input voltage and current space vector and their deviation under normal input voltages (Case 1) and abnormal input voltages (Case 2)

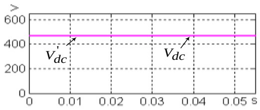

(a) Case 1

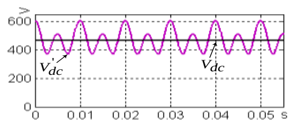

(b) Case 2

Figure 7 Dc-link voltage calculated by (4) and (13) under normal input voltages (Case 1) and abnormal input voltages (Case 2)

B. *Induction Motor Driven by Matrix Converter Operation under Abnormal Input Voltage*

The system configuration of sensorless vector control of induction motor driven by matrix converter is described in Fig. 4. The indirect voltage fed rotor flux oriented control algorithm is applied to the scheme. The principle of the speed controller is to maintain a constant value of the d-axis current while instantaneously changing the q-axis current. As clearly shown in (10), when the rotor flux is held constant, the electromagnetic torque is proportional to the value of q-axis current. Since the voltage-fed model is used, the outputs of the control system are the stator d-q axis voltage references.

The d-q axis components of the reference voltage are described as follows

$$\begin{cases} v^*_q = v'_q + e_q \\ v^*_d = v'_d + e_d \end{cases} \tag{15}$$

where (v'_q, v'_d) are the synchronous reference voltages which the two PI current controller produce, $(e_q, e_d) = (\omega^*_r L_s i^*_{ds}, \omega^*_r \sigma L_s i^*_{qs})$ are two decoupling voltages.

The reference voltages (v^*_q, v^*_d) are then transformed into $\alpha\beta$ axis components which are directly used to derive the desirable magnitude and angular velocity of the output voltage space vector.

Suppose that the reference output phase voltage space vector, at an instant of sampling, has magnitude of V_{om} and angular velocity of θ_o as expressed in (16)

$$\bar{v}_o = V_{om}.e^{j\theta_o} \tag{16}$$

Using (4) and (7), the VSI modulation index m_v is determined as

$$m_v = \frac{\sqrt{3}.V_{om}}{V_{dc}} = \frac{2V_{om}}{\sqrt{3}V_{im}\cos\varphi_i} \tag{17}$$

However, as previously mentioned in IV.A, under abnormal input conditions, the dc-link voltage is no longer constant and vary according to (13). Assuming that value of the dc-link voltage is greater than value of the desirable output line voltage magnitude

$$V'_{dc} \geq \sqrt{3}.V_{om} \tag{18}$$

, then with m_v calculated by (17), the actual value of output phase voltage magnitude that MC can produce is

$$V'_{om} = \frac{1}{\sqrt{3}} m_v.V'_{dc} = V_{om}\frac{|\bar{v}_i|.\cos\varphi'_i}{V_{im}\cos\varphi_i} = K.V_{om} \tag{19}$$

The angular velocity θ_o of the output phase voltage space vector is controlled independently of its magnitude. Therefore, θ_o is exactly obtained regardless of the dc-link voltage variation. As a result, the output phase voltage space vector that MC can obtain is derived as

$$\bar{v}'_o = V'_{om}.e^{j\theta_o} = K.V_{om}e^{j\theta_o} \tag{20}$$

(16) and (20) clearly show that $\bar{v}'_o$ is equal to the reference space vector $\bar{v}_o$ in case of normal input conditions while is different in magnitude in case of abnormal input conditions.

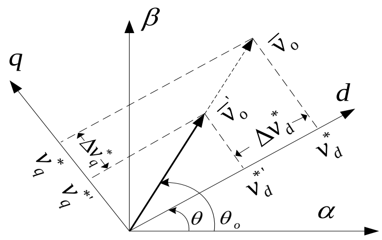

Figure 8 Illustration of actual d-q axis components of a certain reference voltage under abnormal input conditions.

Fig. 8 is used to derive the relationship between output phase voltage space vector variation and the variation of d-q axis components of the reference voltage. It can be seen from Fig. 8 that the d-q axis component variation is proportional to a factor η defined as

$$\eta = \frac{|\bar{v}'_o| - |\bar{v}_o|}{|\bar{v}_o|} = (K-1) \tag{21}$$

Hence, the actual values of d-q axis components of the reference voltage are obtained as

$$\begin{cases} v^{*'}_q = v^*_q + \eta v^*_q = K v^*_q \\ v^{*'}_d = v^*_d + \eta v^*_d = K v^*_d \end{cases} \tag{22}$$

(22) clearly proves that with the input reference voltage components of (v^*_q, v^*_d) in d-q axis, if (18) is satisfied, the actual values that MC can obtain under abnormal input conditions are $K(v^*_q, v^*_d)$. This is equivalent to operation of MC under normal conditions when additional components of $\eta(v^*_q, v^*_d)$ are inserted to the reference components.

As previously mentioned, the reference voltage in d-q axis is used to create appropriate torque to control the induction motor speed. This torque, as described in (10), is proportional to both rotor flux and q-axis current which are respectively controlled by d-axis and q-axis reference voltage components. However, as two components vary according to (22) under abnormal conditions, the actual torque applied to the induction motor by MC will be K^2 times proportional to the reference torque.

C. *Feed-Forward Compensation Strategy*

As discussed in section IV, the dc-link voltage varies during operation of MC under abnormal input conditions. The variation is dependent on the instantaneous magnitude of input phase voltage space vector and the displacement factor as described in (13). The idea of the proposed feed-forward compensation strategy is to calculate the instantaneous value of the dc-link voltage and then adjust the VSI modulation index m_v to an appropriate value. The generalized IDF $\varphi_i^{'}$ which varies with θ_e is held constant by modifying the controllable angular velocity of input current space vector in VSR part as follows

$$\theta_i^{'} = \theta_e - \varphi_i \tag{23}$$

Hence, $\varphi_i^{'} = \theta_e - \theta_i^{'} = \varphi_i$ is always satisfied during abnormal conditions.

The compensation VSI modulation index $m_v^{'}$ is then adjusted according to the dc-link voltage value in (13)

$$m_v^{'} = \frac{\sqrt{3}V_{om}}{V_{dc}^{'}} = \frac{2V_{om}}{\sqrt{3}\left|\bar{v}_i\right| cos\varphi_i} \tag{24}$$

However, as described in (18), the desired output line voltages should not exceed the dc-link voltage value. Otherwise, it would lead to the over modulation and the compensation technique proposed in (23), (24) is no longer satisfied. Therefore, to ensure the effectiveness of the compensation method, a general constraint is proposed as

$$min(V_{dc}^{'}) \geq max(\sqrt{3}.V_{om}) \tag{25}$$

V. Simulation Results

In order to confirm the effectiveness of the feed-forward compensation method, some simulation studies using MATLAB/Simulink to respectively simulate the conventional control strategy, and feed-forward compensation strategy under input voltage condition which contains 10% third harmonic and 20% fifth harmonic. To implement the model of speed sensorless IFOC control of IM driven by MC, a standard 2.2KW, two poles, 380V, 50hz induction motor is used. The induction motor has the following parameter values: R_s =1.79 Ω , R_r =1.8 Ω , L_s =0.0853H, L_r = 0.0853H, L_m = 0.0819H.

The dynamic response of the system is tested with reference to speed change and load variation. The reference speed is set at 60 rad/s in the first second, at 1s a step change happens to set the reference speed at 120 rad/s. Load torque is initially set at zero, step changes in load are applied at 0.5s and 1.5s with values of 3Nm and 7Nm respectively.

Under the same given operating conditions, performances of IM driven by MC without any compensation technique and with feed-forward compensation strategy are illustrated in Fig. 9-Fig. 11. Fig. 9a displays between 1.4s: 1.6s the stator currents in uncompensated system. The stator currents in compensated system with harmonic distortions reduce considerably are shown in Fig. 9b. Effectiveness of the proposed compensation strategy is also demonstrated through improvements in output torque and speed response of IM. As illustrated in Fig. 10a and Fig. 11a, distorted stator currents result in high ripple electromagnetic torque and thus unstable speed of rotor. Fig. 10b and Fig. 11b clearly shows the improvements with very low ripple torque and stable rotor speed when the compensation strategy is applied.

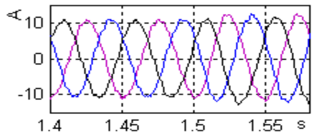

(a) uncompensated system

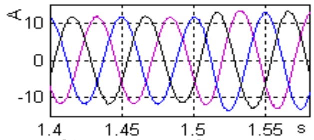

(b) compensated system

Figure 9 Stator currents in uncompensated system and compensated system

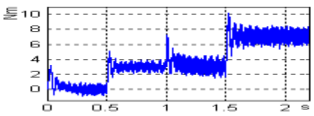
(a) uncompensated system

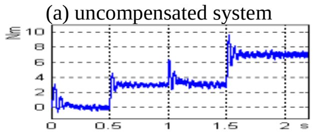
(b) compensated system

Figure 10 Output torque in uncompensated system and compensated system

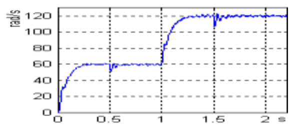
(a) uncompensated system

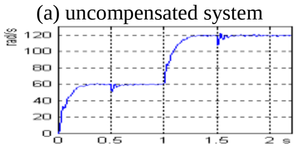
(b) compensated system

Figure 11 Rotor speed in uncompensated system and compensated system

VI. Conclusion

This paper has analyzed the influences of abnormal input voltages to the system of an induction motor driven by a matrix converter. The speed sensorless IFOC is employed as the speed control model for induction motor. To improve the system performance under abnormal input condition, a feed-forward compensation strategy is proposed. Output quality of uncompensated and compensated system has been shown to confirm the effectiveness of the proposed method.

REFERENCES

[1] L. Huber and D. Borojevic, "Space vector modulated three-phase to three-phase matrix converter with input power factor correction," *IEEE Trans. IA,* vol. 31, pp. 1234-1246, Nov/Dec 1995.

[2] F. Blaabjerg, D. Casadei, C. Klumpner, and M. Matteini, "Comparison of two current modulation strategies for matrix converters under unbalanced input voltage conditions," *IEEE Trans,* vol. 49, no. 2, pp. 289-296, April 2002.

[3] D. Casadei, G. Serra, and A. Tani, "Reduction of the input current harmonic content in matrix converters under input/output unbalance," *IEEE Trans*, vol. 45, no. 3, pp. 404-411, June 1998.

[4] P. Nielsen, F. Blaabjerg, and J. K. Pedersen, "Space vector modulated matrix converter with minimized number of switchings and a feed-forward compensation of input voltage unbalanced," *IECON,* vol. 2, pp. 833-839, Jan 1996.

[5] H. Kubota, K. Matsuse, and T. Nakano, "DSP-based speed adaptive flux observer of induction motor," *IEEE Transactions on Industry Applications*, vol. 29, no. 2, pp. 344-348, Mar./Apr. 1993.

[6] K. B. Lee and F. Blaabjerg, "Improved sensorless vector control for induction motor drives fed by a matrix converter using nonlinear modeling and disturbance observer," *IEEE Trans. Energy Convers.*, vol. 21, no. 1, pp. 52–59, Mar. 2006.

[7] K. B. Lee and F. Blaabjerg, "Reduced-order extended luenberger observer based sensorless vector control driven by matrix converter with nonlinearity compensation," *IEEE Trans,* vol. 53, no. 1, Feb. 2006.

[8] M. Montanari, S. M. Peresada, C. Rossi, and A. Tilli, "Speed sensorless control of induction motors based on a reduced-order adaptive observer," *IEEE Trans,* vol. 15, no. 6, Nov. 2007.

Nguyen Khanh Tu Tam received his bachelor's degree in Automatic Control Engineering from the Ho Chi Minh City University of Technology, Vietnam in 2010. He is currently a researcher in Faculty of Electrical and Electronics Engineering, Ho Chi Minh City University of Technology. His research interests mainly include advanced control of electrical machines and power electronics.

Nguyen Van Nho received his M.S. and PhD. degrees in Electrical Engineering from the University of West Bohemia, Czech Republic in 1988 and 1991, respectively. Since 2007, he has been an associate professor of Faculty of Electrical and Electronics Engineering at Ho Chi Minh City University of Technology, Vietnam. He was a postdoctoral at KAIST, Korea in 2001 and was a visiting professor in 2003-2004. His research interests include modeling and control of ac motors, active filters, and PWM techniques. He is a member of the Institute of Electrical and Electronics Engineers (IEEE).

Huynh Thai Hoang was born in Vietnam, in 1974. He received the M.S. and PhD. degrees in Electrical Engineering from Ho Chi Minh City University of Technology, Vietnam in 1999 and 2005, respectively. Since 1996, he has been with Department of Electrical and Electronics Engineering, Ho Chi Minh City University of Technology, Vietnam, where he is currently a Vice Dean. He was with University of Haute Alsace as a post-doc fellow for one year in 2007. His research interests are in the areas of intelligent control and computer vision.